

# Demonstration of a nonmagnetic blazed-grating atomic beam splitter

K. S. Johnson, A. Chu, T. W. Lynn, K. K. Berggren, M. S. Shahriar, and M. Prentiss

Department of Physics, Harvard University, Cambridge, Massachusetts 02138

Received November 28, 1994

We demonstrate a coherent atomic beam splitter for metastable helium atoms, based on the diffraction of atomic matter waves from a blazed phase grating. The beam splitter is created by driving the two transitions of a three-level V system with differentially detuned standing light waves that have a relative spatial phase shift of  $\pi/2$ . The light fields create a potential that is approximately triangular as a function of position in the laser field. Splittings of 38 times the photon momentum have been observed.

For the creation of large-area, high-sensitivity atom interferometers, many atom interferometry applications would benefit from efficient large-angle atomic beam splitters.<sup>1</sup> For example, if the interference of two matter beams is used to produce a nanostructure, a larger angle between the beams leads to a smaller-scale interference pattern, and the overall extent of the pattern increases with increasing beam-splitting efficiency. Moreover, it is often desirable in interferometric applications to avoid static external fields.

A variety of experiments and proposals have addressed the issue of creating a large-angle, efficient atomic beam splitter.<sup>2-8</sup> Recently Pfau and co-workers proposed and demonstrated a magneto-optical beam splitter.<sup>5,9,10</sup> Grimm *et al.* suggested that an efficient beam splitter can be realized by driving a two-level atom with bichromatic standing-wave light fields.<sup>11</sup> In this Letter we demonstrate a large-angle beam splitter based on a three-level V system that does not require an external magnetic field. Splittings of 38 times the photon momentum have been observed. This splitting corresponds to an angular separation of 1.95 mrad and a spatial separation of the two peaks of the atomic wave packet of 3.1 mm in the detection region.

When a plane wave is scattered from a thin phase grating, the far-field momentum distribution  $\Pi(p_z)$  is given by  $\Pi(p_z) \propto |F_z[\exp[-i\phi(z)]]|^2$ , where  $F_z$  is the Fourier transform with respect to  $z$  and  $\phi(z)$  is the phase accumulated by the wave packet during the interaction. In the Raman-Nath regime,  $\hbar\phi(z) \propto \int V(z, t) dt$ . Early demonstrations of the Kapitza-Dirac diffraction of atoms from standing light waves used a single standing light wave that interacted with a two-level atomic system to create a sinusoidal potential energy, which scatters into multiple diffraction orders.<sup>12,13</sup> In contrast, a blazed grating provides a potential and corresponding phase accumulation that is triangular as a function of position and results in a diffraction pattern dominated by two narrow, widely separated peaks. An optical potential that is triangular as a function of position can be used as a blazed grating for matter waves. In the recent work of Pfau and co-workers, a combination of standing light waves and a magnetic field (67 G) was used to create a blazed-grating potential in a three-level V system. We show that such a blazed-grating beam splitter for

three-level atoms can be obtained in the absence of a magnetic field, so long as the two driving fields have different frequencies.

Consider the V system shown in Fig. 1. The two transitions are driven by standing-wave laser fields,  $\Omega_+$  and  $\Omega_-$ , detuned symmetrically above and below the atomic resonance frequency  $\omega_0$ . We assume that  $\Omega_+$  interacts only with the  $|g\rangle \rightarrow |e_+\rangle$  transition and  $\Omega_-$  interacts only with the  $|g\rangle \rightarrow |e_-\rangle$  transition, where  $\Omega_{\pm} = \Omega \cos(kz \pm \chi/2)$ . Here  $\chi$  is the relative spatial phase shift between the standing waves,  $k$  is the wave number of the light,  $z$  is the position in the standing wave, and  $\Omega$  is the peak Rabi frequency.<sup>14</sup> The interaction Hamiltonian, in the  $|e_+\rangle, |e_-\rangle, |g\rangle$  basis and in the rotating frame, is

$$H = \hbar/2 \begin{bmatrix} \Delta & 0 & -\Omega_+ \\ 0 & -\Delta & -\Omega_- \\ -\Omega_+ & -\Omega_- & 0 \end{bmatrix}. \quad (1)$$

Here  $\Delta$  is the difference between the frequencies of the two driving fields. For a resonant condition  $\Omega = \sqrt{2}\Delta/\sin(\chi)$ , and for a particular spatial phase shift  $\chi = \pi/2$ , the dressed state adiabatically connected to  $|g\rangle$  as  $\Omega \rightarrow 0$  has an energy that is nearly triangular as a function of position, as shown in Fig. 2(a). Thus, if an atom in  $|g\rangle$  enters a Gaussian laser profile slowly, the atom will follow adiabatically into the dressed state associated with the triangular potential. Although the resonant condition that provides the most triangular potential will not be met everywhere in the Gaussian intensity profile, the efficiency of the splitting is not seriously compromised. An atom in the ground state of a V system will diffract from the

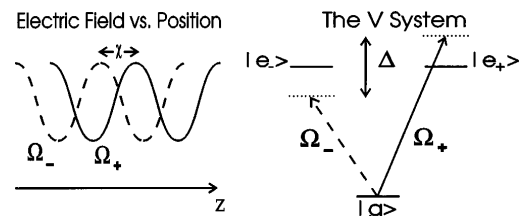


Fig. 1. Schematic of the V system.  $\Omega_-$  interacts only with the  $|g\rangle \rightarrow |e_-\rangle$  transition, and  $\Omega_+$  interacts only with the  $|g\rangle \rightarrow |e_+\rangle$  transition. The spatial dependence of the driving fields is given by  $\Omega_{\pm} = \Omega \cos(kz \pm \chi/2)$ , the differential detuning is  $\Delta$ , and  $\chi$  is the spatial phase shift between the two standing waves.

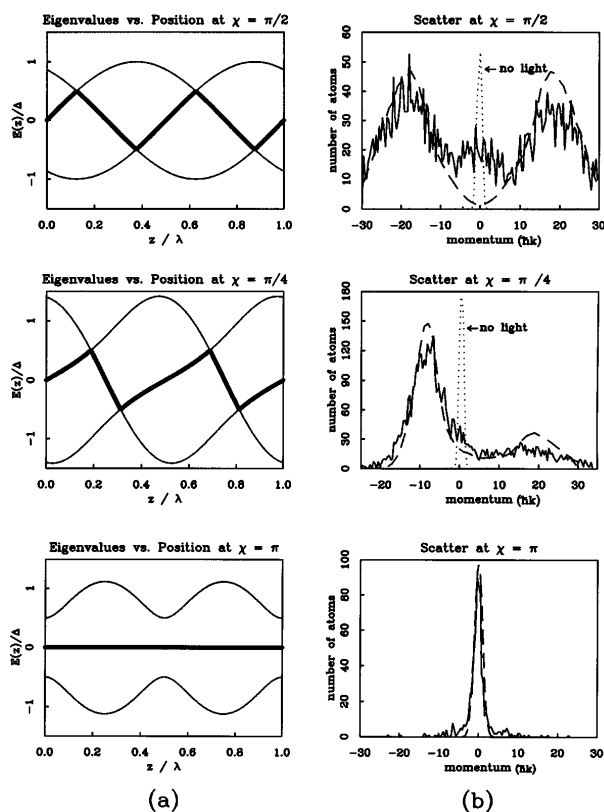


Fig. 2. (a) Eigenvalues as a function of position in the laser field for phases of  $\pi/2$ ,  $\pi/4$ , and  $\pi$ . In each case the central, darker energy level is connected adiabatically to  $|g\rangle$  as  $\Omega \rightarrow 0$ . (b) The dashed curves correspond to the theoretical far-field momentum distributions calculated by integrating the Schrödinger equation; the dotted curves represent the atomic beam in the absence of laser interaction; the solid curves correspond to the experimental data.

blazed grating, resulting in two symmetric narrow peaks, as shown in Fig. 2(b). We note that in the cases of experimental interest here, the atoms do not move significantly along  $\hat{z}$  during the interaction (Raman-Nath regime). If the interaction time is short enough (but long enough to satisfy the adiabaticity criterion), then the effect of spontaneous emission will be small, and the beam splitting will be coherent.

When the two standing waves have a phase shift other than  $\pi/2$ , the eigenenergy associated with  $|g\rangle$  can have a nontriangular position dependence. For example, as pointed out by Pfau and co-workers, at a phase of  $\pi/4$  a sawtooth potential can be created for appropriate values of  $\Delta$  and  $\Omega$ . The far-field momentum distribution for atoms scattered from this potential is shown in Fig. 2(b). One can see that most of the atomic wave packet is deflected through a small angle in one direction, while a small portion of the wave packet is deflected through a large angle in the opposite direction; although it yields no net deflection for the center of mass, this potential acts somewhat like a mirror. A phase of  $\chi = 0$  or  $\pi$  gives rise to a translationally invariant potential for the dressed state connected to  $|g\rangle$ . This translational invariance is insensitive to both the absolute and relative values of  $\Delta$  and  $\Omega$ . This potential is the analog of a flat glass plate in light optics; such a potential should not deflect

the atomic beam. We use this behavior at  $\chi = 0, \pi/4$  to confirm the signature of the three-level interaction.

The experimental setup is shown schematically in Fig. 3. Most of the apparatus has been described previously.<sup>8,15</sup> The experiment is performed with a thermal effusive beam of metastable helium atoms that travel with an average velocity of 1800 m/s in the  $\hat{y}$  direction. The atomic beam is collimated to  $2\hbar k$  in the  $\hat{z}$  direction. The triplet metastable helium atoms interact with light at a wavelength of  $1.083 \mu\text{m}$  resonant with the  $2S_3^3$  to  $2^3P_1$  transition.

The light is obtained from a lanthanum-neodymium-hexaluminate (LNA) laser pumped by an argon-ion laser. The laser is frequency-locked to the atomic transition by means of saturation spectroscopy in a rf helium discharge cell. To transform the  $J_g = 1 \rightarrow J_e = 1$  transition into a closed V system we first optically pump all the ground-state atoms into the  $m_j = 0$  sublevel. An optical pumping beam propagates along  $\hat{x}$  and is  $\pi$  polarized along  $\hat{z}$ . A 0.3-G quantizing magnetic field is applied along  $\hat{z}$  in the optical pump and interaction regions. The fields in the  $\hat{x}$  and  $\hat{y}$  directions are less than 0.02 G throughout the interactions. After leaving the optical pumping region the atoms travel approximately 3 mm before entering the beam-splitter interaction region.

The two standing waves are derived from a single laser beam split by a polarizing beam-splitter cube (PBS1). Two acousto-optic modulators (AOM1 and AOM2) are used to shift the two light beams symmetrically above and below the atomic resonance. After recombination of the light beams on a second polarizing beam splitter (PBS2), the shifted laser beams are coupled into the orthogonal modes of a single-mode, polarization-maintaining optical fiber. A half-wave plate is used to align the linear polarizations with the axes of the optical fiber. After passing the optical fiber, the overlapping beams are collimated to a waist of 2.3 mm. A quarter-wave plate transforms the two orthogonal linear polarizations into  $\sigma_+$  and  $\sigma_-$  polarized light. In the absence of spontaneous emis-

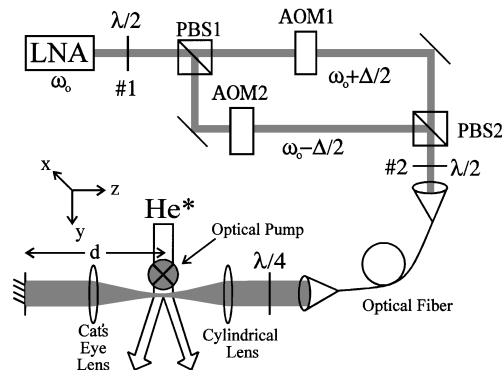


Fig. 3. Schematic of experimental apparatus.  $\lambda/2$  wave plate 1 and the first polarizing beam splitter (PBS1) are used to control the intensity of the light that goes to each acousto-optic modulator (AOM1 and AOM2). The laser beams then are recombined on PBS2 and coupled into a polarization-maintaining single-mode optical fiber. The  $\lambda/4$  plate transforms the linear polarized light into the two orthogonal circular polarization states before the light is focused onto the atomic beam. A cat's-eye retroreflector creates the standing wave.

sion during the beam-splitter interaction, such a laser configuration reduces the  $J_g = 1 \rightarrow J_e = 1$  transition to a closed three-level V system. A 15-cm focal-length cylindrical lens is used to focus the beam to a waist of 23  $\mu\text{m}$  in the  $\hat{y}$  direction at the atomic beam.

A cat's-eye retroreflector is then used to establish a standing wave. We monitor the quality of the standing wave by maximizing the intensity of the light that couples back into the fiber and also by studying the diffraction of atoms from a single standing wave. The spatial phase shift between the  $\sigma_+$  and  $\sigma_-$  standing waves is determined by the evolution of the different frequencies of light through the cat's-eye retroreflector. In terms of differential detuning  $\Delta$  and the distance from the atomic beam to the back mirror  $d$ , the spatial phase shift is given by  $\chi = 2\pi\Delta d/c$ , where  $c$  is the speed of light.

The spatial distribution of the atoms is detected 1.6 m downstream by a position-sensitive microchannel plate detector. We obtain the time-of-flight selection by pulsing the source and the detector, which yields a  $v/\delta v$  value of 4.5. The metastable singlet helium atoms pass through the interaction region undeflected and can be subtracted from the data, given the measured fraction of singlets (approximately 10%). The metastable triplet atoms interact with the excitation fields for 26 ns; this interaction time is shorter than the 99.5-ns natural lifetime of the atomic excited state and yields less than a 12% probability of spontaneous emission.

Figure 2(a) shows the dressed-state energies as a function of position in the standing wave, and Fig. 2(b) shows the predicted far-field scatter patterns and the experimental data. The energies come from a diagonalization of the Hamiltonian of Eq. (1). The ratio of  $\Delta$  and  $\Omega$  is chosen to satisfy the resonant condition for  $\chi = \pi/2$  and  $\chi = \pi/4$ . The dressed state adiabatically connected to  $|g\rangle$  is the darker, central energy level in each case.

The results of our calculations for the final momentum distributions are given in Fig. 2 by the dashed curves. To calculate the expected final momentum distribution, we integrate the Schrödinger equation numerically in the momentum state basis, starting with a plane wave of zero transverse momentum. During the integration we ignore changes in the transverse momentum; we have determined explicitly that inclusion of the transverse kinetic energy term in the Hamiltonian does not significantly alter the final momentum distribution. The results of the calculations include the spatial extent of the atomic beam, the initial transverse momentum width, the effect of optical pumping, and the longitudinal velocity distribution.

The data for spatial phases of  $\pi/2$ ,  $\pi/4$  and  $\pi$  represent 0.75, 0.5, and 0.25 h of integration time, respectively. When the time-of-flight selection is set for the narrowest velocity distribution, the count rate for the atomic beam is roughly 1.5 Hz. In the experimental data, the metastable singlets have been subtracted from the raw data to show the beam-splitting effect more clearly. At  $\chi = \pi/2$ , the differential detuning was set to 250 MHz, while the laser power was 7 mW per individual traveling wave. We believe that the residual counts in the central region

of the  $\chi = \pi/2$  data are caused by slight imperfections in optical pumping, quantization angle, and impure polarization of the standing waves, which we have not included in our calculation. The data shown correspond to a splitting of 38 times the photon momentum. At  $\chi = \pi/4$  the differential detuning was 225 MHz, while the intensity in each traveling wave was 6 mW. This intensity corresponds to a Rabi frequency below the resonant Rabi frequency. Thus we do not intend a direct comparison between the data taken with  $\chi = \pi/4$  and  $\chi = \pi/2$ ; rather the  $\chi = \pi/4$  data represent a verification of the blazed-grating interaction. At  $\chi = \pi$  the differential detuning was 250 MHz and the intensity was 5 mW, but the potentials and resultant scatter are insensitive to the specific parameters for this spatial phase shift. The dotted curves in Fig. 2(b) show the undeflected atomic beam. In summary, we have explored and confirmed all three signatures of the phase dependence for the nonmagnetic blazed-grating beam splitter.

This research was funded in part by National Science Foundation grant PHY-9312572 and U.S. Office of Naval Research grant ONR-N0014-91-J-1808. T.W. Lynn acknowledges support from the Rowland Fund. K.S. Johnson is an AT&T Graduate Fellow. A. Chu is a National Science Foundation Graduate Fellow. We warmly thank John Lawall and Li You for fruitful discussions and helpful suggestions.

## References

1. See, for example, the special issue on optics and interferometry with atoms, *Appl. Phys. B* **54**, 319–485 (1992).
2. M. Weitz, B. C. Young, and S. Chu, *Phys. Rev. Lett.* **72**, 2563 (1994).
3. D. S. Weiss, B. C. Young, and S. Chu, *Phys. Rev. Lett.* **70**, 2706 (1993).
4. M. Kasevich and S. Chu, *Phys. Rev. Lett.* **67**, 181 (1991).
5. T. Pfau, Ch. Kurtsiefer, C. S. Adams, M. Siegel, and J. Mlynek, *Phys. Rev. Lett.* **71**, 3427 (1993).
6. T. Sleator, T. Pfau, V. Balykin, O. Carnal, and J. Mlynek, *Phys. Rev. Lett.* **68**, 1996 (1992).
7. L. S. Goldner, C. Gerz, R. J. C. Spreeuw, S. L. Rolston, C. I. Westbrook, W. D. Phillips, P. Marte, and P. Zoller, *Phys. Rev. Lett.* **72**, 997 (1994).
8. J. Lawall and M. G. Prentiss, *Phys. Rev. Lett.* **72**, 993 (1994).
9. T. Pfau, C. S. Adams, and J. Mlynek, *Europhys. Lett.* **21**, 439 (1993).
10. C. S. Adams, T. Pfau, Ch. Kurtsiefer, and J. Mlynek, *Phys. Rev. A* **48**, 2108 (1993).
11. R. Grimm, J. Soding, and Yu. B. Ovchinnikov, *Opt. Lett.* **19**, 658 (1994).
12. P. E. Moskowitz, P. L. Gould, S. R. Atlas, and D. E. Pritchard, *Phys. Rev. Lett.* **51**, 370 (1983).
13. P. L. Gould, G. A. Ruff, and D. E. Pritchard, *Phys. Rev. Lett.* **56**, 827 (1986).
14. Although the difference in frequency  $\Delta$  of the two standing waves implies a difference  $\delta k = \Delta/c$  in their  $k$  vectors, this difference is negligible. For cases of experimental interest,  $\delta k/k \sim 10^{-7}$ .
15. J. Lawall, "A coherent atomic beamsplitter based on adiabatic passage," Ph.D. dissertation (Harvard University, Cambridge, Mass., 1993).